Journal of Sedimentary Research

Journal of Sedimentary Research, 2016, v. 86, 749–761
Research Article
DOI: http://dx.doi.org/10.2110/jsr.2016.49

PROPORTION OF GLACIALLY TO FLUVIALLY INDUCED QUARTZ GRAIN MICROTEXTURES ALONG THE CHITINA RIVER, SE ALASKA, U.S.A.

DUSTIN E. SWEET AND DAVID K. BRANNAN
Department of Geosciences, Texas Tech University, Lubbock, Texas 79409, U.S.A.
e-mail: dustin.sweet@ttu.edu

ABSTRACT: **Certain micrometer-scale fractures, or microtextures, on grain surfaces are the result of specific transport processes. Accordingly, these transport-induced microtextures are used to infer depositional setting in ancient deposits. Multiple transport histories complicate the microtextural record because modification of grain surfaces can reduce or eliminate the signal of earlier transport episodes. This study utilizes scanning electron microscopy to analyze surface microtextures to assess the role of fluvial overprint on glacially derived grains along ~ 188 km of the proglacial Chitina River, SE Alaska. Results indicate that occurrence frequency of glacially induced microtextures (i.e., straight and curved grooves, deep troughs, and crescentic gouges) negatively correlates to distance downstream, yet these microtextures persist in every sample. Conversely, occurrence frequency of fluvially induced microtextures (i.e., v-shaped cracks and edge rounding) positively correlate to distance downstream. At least in the Chitina River watershed, the ratio of fluvially to glacially induced microtextures (F/G ratio) generally records physiographic variation, including increase in fluvial signal after a major tributary confluence, and decrease downstream from the intersection of valley glaciers. These results suggest that analysis of quartz grain microtextures in ancient fluvial deposits can be used to infer glacial influence when other diagnostic sedimentologic indicators of glaciation are lacking. Other potential uses for the proxy may exist, but need to be assessed after other modern proglacial systems are studied, including: 1) estimates of distance to paleo–ice margins using the respective downstream trends of glacially or fluvially induced microtextures, and 2) paleogeography of ancient glacio-fluvial systems through F/G ratio analysis.**

INTRODUCTION

Scanning electron microscopy (SEM) analysis of quartz grain surface features has been utilized since the 1960s to ascertain grain transport history after liberation from provenance rock to final deposition (e.g., Krinsley and Takahashi 1962; Krinsley and Donahue 1968; Krinsley and Doornkamp 1973; Mahaney 2002). Although SEM analysis of quartz grain surfaces is not capable of inferring all styles of transport, a few processes and environments can be determined from surface microtextures and their frequency of occurrence. For example, stick–slip flow of wet-based glaciers can create internal shear (e.g., Fischer and Clarke 1997), allowing grain-to-grain *stylus* contact along shear planes resulting in a specific suite of microtextures, whereas aqueous percussion transport produces a specific suite of grain-to-grain *impact* microtextures on grain surfaces (Krinsley and Doornkamp 1973; Mahaney and Kalm 2000; Mahaney 2002; Whalley and Langway 1980).

Many SEM microtexture studies have documented multiple phases of transport through crosscutting relationships of microtextures. For example, Jackson (1996) observed v-shaped cracks attributed to fluvial saltation atop surfaces that exhibit glacially induced stylus microtextures in fluvial sands collected approximately 10 km downstream from the terminal moraine. In a later study, Mahaney and Kalm (2000) documented glacially induced stylus microtextures with scarce percussion-induced microtextures in Pleistocene till, yet approximately 100 km away in associated proglacial fluvial deposits, percussion-induced microtextures were abundant and stylus microtextures were absent. These two case studies indicate that fluvial transport modifies grains that exhibit older glacial transport histories. However, no study to date has systematically assessed the overall abundance and survivability of glacially induced microtextures during progressive fluvial transport. We pose three questions that remain unanswered and address the significance of each below.

How far downstream can glacially induced microtextures survive in a fluvial system while undergoing surface modification during traction and saltation? If glacially induced microtextures remain within a proglacial fluvial system, then SEM analysis of quartz grains can be administered to decipher between ancient proglacial and nonglacial, coarse-grained fluvial strata. This is especially important as facies models of coarse-grained fluvial systems differentiate poorly between nonglacial and proglacial systems. Some facies models of braided river systems are based entirely on glacially derived systems (Boothroyd and Ashley 1975; Boothroyd and Nummendal 1978) even though the models are argued to apply to all braided river systems (e.g., Miall 1978; Boothroyd and Nummendal 1978). More recent assessments of proglacial river systems suggest that large and abundant flood facies provide evidence to differentiate proglacial from nonglacial braided rivers (e.g., Maizels 1993, 1997; Marren 2002); however, this argument is not necessarily diagnostic of ice because floods occur in rivers of all types and abundance is a matter of preservation.

Published Online: July 2016
 1527-1404/16/086-749/$03.00

Does the degree of fluvial modification correspond to distance downstream? If glacially induced microtextures are systematically modified downstream by fluvial saltation and traction, then the relationship between distance downstream and relative abundance of glacially to fluvially induced microtextures may potentially estimate paleo–ice margins. Margins of ancient ice are most commonly assessed by the location of moraines. However, glacial deposits are typically incomplete because glacial advance often erodes previously deposited sediments (e.g., Johnson and Hansel 1999). Thus, potential microtextural trends derived from modern proglacial rivers may provide an alternative way to estimate locations of paleo–ice margins when sedimentologic indicators are absent.

Can the relationship of fluvially to glacially induced microtextures record actual changes in river physiography in a modern proglacial system? If glacially induced microtextures are modified according to the distance that a grain is subjected to saltation and traction, then the ratio of fluvially to glacially induced microtextures may potentially reflect changes in river physiography, such as glacial or fluvial confluences. For example, major tributary confluences should increase the number of grains that were subjected to fluvial transport and the ratio should increase. Alternatively, if valley glaciers are intersected, then more grains with solely glacial transport should be supplied to the river and the ratio should decrease. Therefore, applying this ratio to ancient rivers may help reveal specific paleogeographic components of past proglacial systems.

This study uses SEM to examine quartz grains recovered from the Chitina River of SE Alaska and seeks to answer the above outstanding questions. To observe downstream variation in microtextures, 1,076 quartz grains were analyzed from 40 samples, beginning at the terminal moraine of the Chitina Glacier and extending to the Chitina–Copper river confluence approximately 188 km downstream. The analysis documents change in the abundance of glacially induced stylus microtextures (i.e., grooves, troughs, and gouges) observed on grain surfaces, and fluvial percussion-induced microtextures (i.e., v-shaped cracks and edge rounding) versus distance downstream. Results indicate that glacially induced microtextures are liberated into the fluvial system and persist downstream, but are progressively modified by traction and saltation.

Surface Microtextures: Background

Quartz grain microtextures record surface modification resulting from grain-to-grain collision during transport after the initial grain liberation to final deposition. Accordingly, SEM analysis of grain surfaces has been used since the 1960s to affiliate quartz grain characteristics with geologic processes (e.g., Krinsley and Takahashi 1962; Krinsley and Donahue 1968; Krinsley and Doornkamp 1973; Mahaney 2002). Previous extensive studies have demonstrated that only a few microtextural suites reflect distinct sedimentary transport processes (e.g., Biederman 1962; Porter 1962; Krinsley and Donahue 1968; Campbell and Thompson 1991; Mahaney and Kalm 2000; Mahaney 2002) whereas many individual microtextures are produced from different transport processes. Similar microtextures imparted by dissimilar transport methods are of little significance for determining depositional environments (Brown 1973; Campbell and Thompson 1991). However, transport-unique microtextures can be used in conjunction with local geology and other sedimentologic observations to infer depositional environment (e.g., Krinsley and Donahue 1968; Campbell and Thompson 1991; Mahaney 2002; Sweet and Soreghan 2010; Keiser et al. 2015).

As certain microtextures on grain surfaces are created by specific transport processes, Campbell and Thompson (1991) suggested that microtextures could be divided into suites based on imparted surface features. Sweet and Soreghan (2010) further argued that microtextures can be grouped into three genetic categories of transport style defined as sustained shear stress, percussion, and polygenetic (Table 1). Thus, the particular suite of microtextures observed on grain surfaces may reflect the transport style imposed on the grains, and in conjunction with other geologic relationships, specific processes of depositional environment can be assessed.

Sustained-Shear-Stress Microtextures

In viscous media, such as ice or debris flows, grain-to-grain contact along existing shear planes can result in one grain stylizing microtextures onto another grain. Microtextures imparted through a grain stylus include straight and curved grooves, deep troughs, and crescentic gouges (Mahaney 2002; Sweet and Soreghan 2010). Mechanically upturned plates are recorded in grains recovered from glacial deposits (Mahaney and Kalm 2002; Mahaney 2002) and were incorporated in the original sustained-shear-stress suite defined by Sweet and Soreghan (2010). Mechanically upturned plates also have been reported on eolian grains (e.g., Krinsley and Donahue 1968; Krinsley and Doornkamp 1973), thus in this study we have chosen to not include mechanically upturned plates in this microtextural suite.

Wet-based, temperate glaciers entrain sediment through a variety of processes, but often through melt–freeze processes at the basal surface (Alley et al. 1997). Basal melting coupled with increased pore pressure in subglacial sediment allows faster slip rates along the basal surface of the glacier. Conversely, freezing of the basal surface to the underlying surface results in internal shear—referred to as stick–slip motion (e.g., Fischer and Clarke 1997). Wet-based glaciers produce quartz grains with relatively abundant sustained-shear-stress microtexture frequency occurrence (Whalley and Langway 1980; Campbell and Thompson 1991; Mahaney and Kalm 2000; Mahaney 2002). Continental ice sheets also produce sustained-shear-stress microtextures, but typically at a lower frequency of occurrence (e.g., Mahaney et al. 1988; Mahaney et al. 1996; Kirshner and Anderson 2011; Immonen et al. 2014; Witus et al. 2014), presumably because cold-based glaciers have lower basal slip rates with relatively weak entrainment of sediment compared to wet-based glaciers (e.g., Cuffey et al. 2000). When sustained-shear-stress microtextures have been observed in significant quantities, a glacial origin is the most common system studied or inferred, especially if other corroborating geologic relationships exist (Krinsley and Takashi 1962; Whalley and Langway 1980; D'Orsay and van de Poll 1985; Campbell and Thompson 1991; Mahaney et al. 1996; Mahaney and Kalm 1995, 2000; Mahaney et al. 2001a; Mahaney 2002; Strand et al. 2003; Van Hoesen and Orndorff 2004; Sweet and Soreghan 2010; Kirshner and Anderson 2011; Witus et al. 2014; Immonen et al. 2014; Keiser et al. 2015).

Other processes or environments producing grain-to-grain contact under enough shear to stylize grain surfaces include structural shear zones (Helland and Diffendal 1993) and high-viscosity debris flows (Mahaney 2002). A study that assessed microtextures on grains recovered from *in situ* tills versus paraglacial debris flows found that the occurrence of microtextures in the two sample suites was statistically insignificant (Curry et al. 2009). Thus, it seems that in this case, debris-flow transport did not meaningfully overprint the original glacial-transport microtexture signal. Nevertheless, the study provides a cautionary note on the need to incorporate other geologic relationships into environmental interpretations using sustained-shear-stress microtextures.

Percussion Microtextures

In low-viscosity media, such as air or water, saltating sand grains result in grain-on-grain impact and that percussion produces edge rounding and v-shaped cracks indicative of impacts during saltation and traction (Table 1; Krinsley and Donahue 1968; Margolis 1968; Campbell and Thompson 1991; Mahaney and Kalm 2000; Mahaney 2002; Mahaney and Dohm 2011). Depositional environments producing percussion microtextures

TABLE 1.—*Classification of transport-induced microtextures on quartz grain surfaces*.

Microtexture Nomenclature	Characteristics[1]	Process of Microtexture Formation[2]	Inferred Transport (This Study Specific)	Selected Reference(s)
Edge rounding	Rounded edges on grains	Percussion	Fluvial	Whalley and Langway 1980; Campbell and Thompson 1991; Mahaney and Kalm 1995, 2000; Mahaney 2002
V-shaped cracks	V-shaped fractures of variable size and depth on grain surface	Percussion	Fluvial	Margolis 1968; Krinsley and Donahue 1968; Campbell and Thompson 1991; Mahaney and Kalm 1995, 2000
Abrasion features	Rubbed or worn-down grain surfaces	Polygenetic	Non-specific	Mahaney and Kalm 1995, 2000; Mahaney 2002; Mazzullo and Ritter 1991
Arc-shaped steps	Arcuate fractures on grain surfaces, typically depths greater than micrometers	Polygenetic	Non-specific	Campbell and Thompson 1991; Mahaney and Kalm 1995, 2000; Mahaney 2002
Breakage blocks	Space represented by removal of block of variable size on grain surface	Polygenetic	Non-specific	Campbell and Thompson 1991; Mahaney and Kalm 1995; Mahaney 2002
Mechanically Upturned Plates	Partially torn-loose plates from the mineral surface.	Polygenetic	Non-specific	Krinsley and Doornkamp 1973; Mahaney and Kalm 2000; Mahaney 2002
Conchoidal fractures	Smooth curved fractures with ribbed appearance	Polygenetic	Non-specific	Campbell and Thompson 1991; Mahaney and Kalm 1995; Mahaney 2002
Fracture faces	Large, smooth, and clean fractures of at least 25% of grain surface	Polygenetic	Non-specific	Mahaney 2002
Linear steps	Widely spaced ($>$ 5 μm) linear fractures on grain surface	Polygenetic	Non-specific	Campbell and Thompson 1991; Mahaney and Kalm 1995; Mahaney 2002
Sharp angular features	Distinct sharp edges on grain surface	Polygenetic	Non-specific	Campbell and Thompson, 1991; Mahaney and Kalm 1995; Mahaney 2002
Subparallel linear fractures	Linear fractures on grain surface, typically $<$ 5 μm spacing	Polygenetic	Non-specific	Helland and Diffendal 1993; Mahaney and Kalm 1995, 2000; Mahaney 2002
Crescentic Gouges	Crescent-shaped gouges on grain, typically $>$ 5 μm deep	Sustained shear stress	Glacial	Campbell and Thompson 1991; Mahaney et al. 1988, Mahaney 2002
Deep Troughs	Grooves $>$ 10 μm deep	Sustained shear stress	Glacial	Mahaney and Kalm 1995, 2000; Mahaney 2002
Straight Grooves	Linear grooves on mineral surface typically $<$ 10 μm deep	Sustained shear stress	Glacial	Helland and Diffendal 1993; Mahaney and Kalm 1995, 2000; Mahaney 2002
Curved Grooves	Curved grooves on mineral surface typically $<$ 10 μm deep	Sustained shear stress	Glacial	Helland and Diffendal 1993; Mahaney and Kalm 1995, 2000; Mahaney 2002

[1] Descriptions from Mahaney (2002).
[2] Classifications from Sweet and Soreghan (2010), except mechanically upturned plates modified.

include fluvial (Helland and Diffendal 1993; Mahaney and Kalm 2000; Sweet and Soreghan 2010), eolian (Al-Saleh and Khalaf 1982; Mazzullo 1987; Mahaney and Andres 1991, 1996; Malhame and Hesse 2015), and near-shore marine systems (Biederman 1962; Krinsley and Donahue 1968; Margolis 1968; Campbell and Thompson 1991; Mahaney and Dohm 2011; Hossain et al. 2014). The diversity of environments with saltation and traction transport of sand requires integration of other independent geologic evidence for depositional environmental interpretation (Campbell and Thompson 1991; Mahaney 2002). For example, to infer percussion-induced microtextures resulting from transport in an ancient fluvial system, other geologic or sedimentologic observations must be inconsistent with eolian and near-shore marine systems and consistent with fluvial deposition (cf. Campbell and Thompson 1991; Sweet and Soreghan 2010; Malhame and Hesse 2015).

Polygenetic Microtextures

The majority of transport-induced microtextures observed on quartz grain surfaces have been observed in a variety of depositional systems under different styles and transport media (e.g., Mahaney 2002). Resulting polygenetic microtextures include conchoidal fractures, mechanically upturned plates, step fracturing, and lineations (Table 1). A wide range of environments impart polygenetic microtextures onto grain surfaces, including burial or tectonic stress (Mazzullo and Ritter 1991), glacial stress (Mahaney and Kalm 2000; Mahaney 2002), mass-flow, matrix shearing (Mahaney 2002), bed-load grain contact during eolian and aqueous saltation (Mahaney and Andres 1991, 1996; Helland and Diffendal 1993; Mahaney and Kalm 2000; Sweet and Soreghan 2010; Mahaney and Dohm 2011), comet impacts (Mahaney 2002), and shrink–swelling of soil (Mahaney et al. 2001b, 2001c; Sweet and Soreghan 2008). Thus, SEM

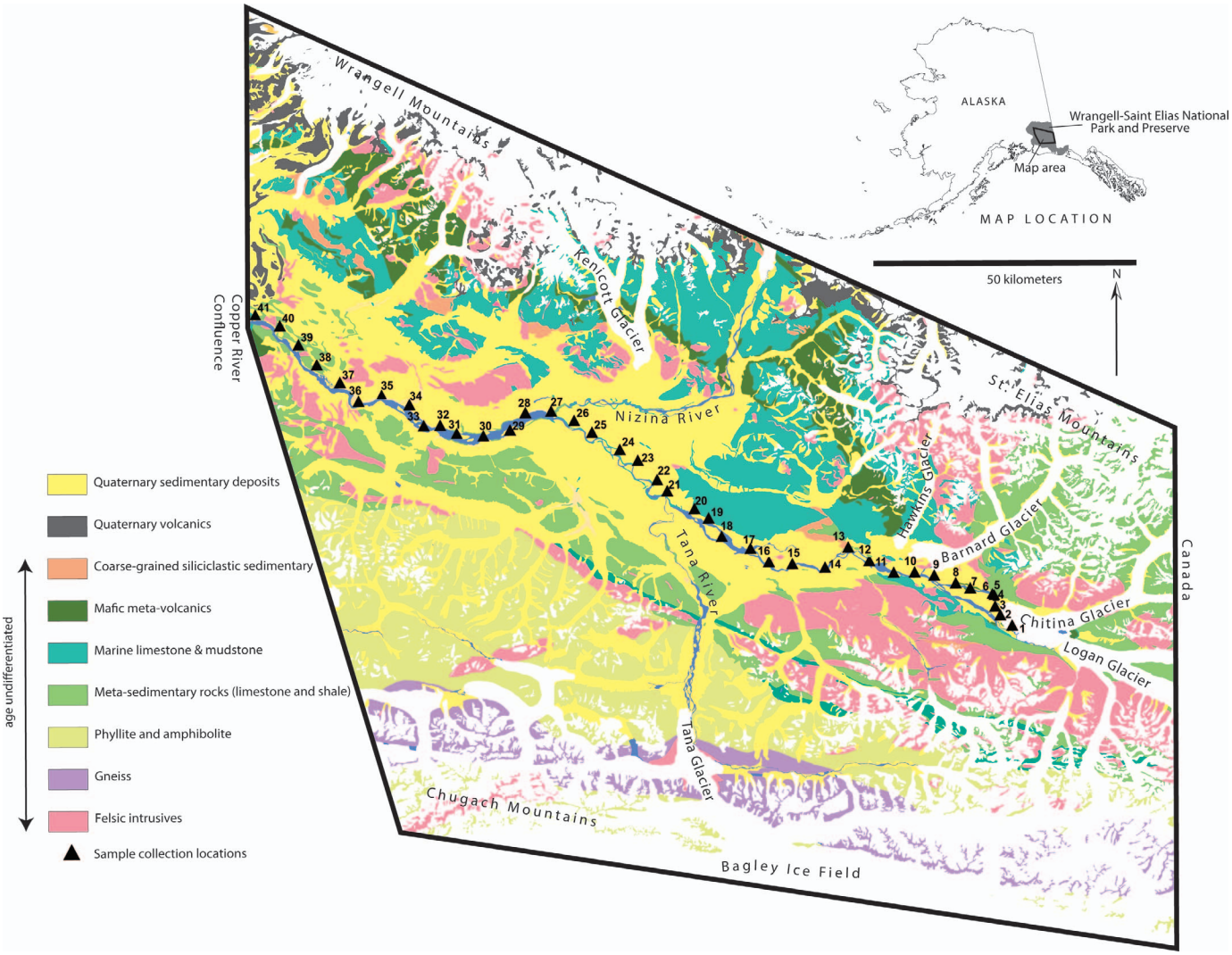

FIG. 1.—Simplified geologic map of the region surrounding the Chitina River, SE Alaska (modified from Richter et al. 2006). Black triangles indicate sampling locations along the Chitina River. For clarity, CR has been omitted from sampling terminology, but is retained elsewhere. Rock units are grouped into potential source lithotypes supplying sediment to the Chitina River. Also, note locations of Tana and Nizina rivers and Barnard and Hawkins glaciers as they are often referred to in text.

polygenetic microtextures are of limited use for determining specific transport process (Brown 1973).

GEOLOGIC AND GEOMORPHOLOGIC BACKGROUND

Regional Tectonic History

The Chitina River is located in the Wrangell–St. Elias National Park and Preserve in SE Alaska and is surrounded by the Chugach Mountains to the south and the Wrangell Mountains to the north (Fig. 1). The Chugach and Wrangell mountains are cored chiefly by metamorphic and igneous assemblages with minor sedimentary deposits ranging in geologic age from Permian to Quaternary (MacKevett 1978). The region is mainly the product of accretion of allochthonous terranes along the continental margin, resulting in a complex tectonic history (Nokleberg et al. 1985).

Terranes composing the Wrangell–St. Elias region include the Wrangellia, Windy, Alexander, Yakutat, Chugach, and Price William composite terranes (Nokleberg et al. 1994). The Wrangellia composite terrane (WCT) and Chitina arc compose the exposed bedrock of the Chitina River watershed (Trop et al. 2002; Richter et al. 2006). The Chitina arc formed along the southern margin of the WCT during the initial collision of the Chugach and Wrangellia terranes approximately 170–150 Ma (Nokleberg et al. 1985, 1994). Upper Jurassic plutonic and metaplutonic rocks constitute the Chitina arc and surround the headwaters of the Chitina River (Fig. 1). The Chitina arc is the main source of first-cycle sediment in the Chitina River and is the dominant provenance for quartz sand.

The surrounding Wrangell and Chugach mountains contain multiple sedimentary or metasedimentary formations in the Chitina River watershed that could provide second-cycle sediment with potentially an inherited microtextural history. The units are chiefly mudstone and carbonate, but a few coarse-grained, siliciclastic lithotypes occur (Trop et al. 2002). Given that these lithotypes are volumetrically minor and exposed predominantly in the lower reaches of the Chitina River (Fig. 1; Mackevett 1978; Nokleberg et al. 1994; Trop et al. 2002), second-cycle sand is not considered a concern.

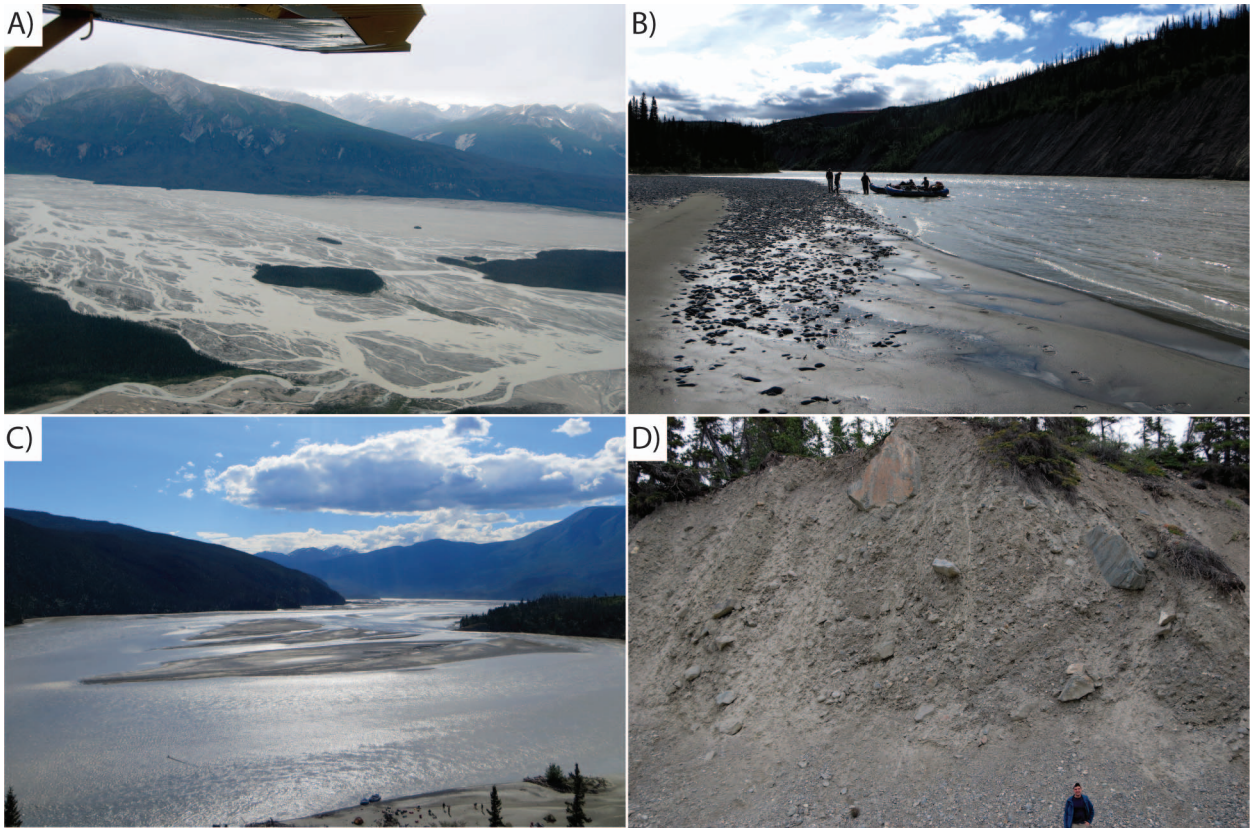

FIG. 2.—**A)** Photograph demonstrating the abundant tightly braided channels characteristic of the upper Chitina River. The small tributary in the lower left is fed by meltwater from the Barnard Glacier. **B)** Photograph of sample site CR-25 demonstrating single channel and transverse bars characteristic of the Chitina River between the Tana and Nizina tributary confluences. **C)** View of the anastomosing channels in the lower reaches of the Chitina River downstream of Nizina River confluence. **D)** Photograph of the terminal moraine of the Chitina Glacier. Sample CR-1 was taken at this locality.

Pleistocene Deposits in the Chitina River Watershed

Pleistocene deposits housed in the Chitina River watershed mainly record glacial outwash, till, and glacio-lacustrine environs from previous glacial episodes (Fig. 1; MacKevett 1978; Richter et al. 2006). The glacio-lacustrine units are largely silt with minor sands and occur predominantly along the single-channel stretch of the Chitina River between the Tana River and the Nizina River confluences (Fig. 1). From the Chitina Glacier terminus to the Hawkins Glacier (Fig. 1), the surrounding Quaternary deposits are Holocene stream gravels; however, downstream of the Hawkins Glacier, Pleistocene glacial drift surrounds the active Chitina River floodplain (Richter et al. 2006). Thus, upstream of the Hawkins Glacier there is very little chance to recycle Pleistocene deposits, yet downstream of the Hawkins Glacier a potential steady background of recycled Pleistocene deposits exists.

Physiography and Hydrology of the Chitina River

The Chitina River is part of the larger Copper River basin watershed, which encompasses approximately 53,350 km^2. In the mid-1980s, approximately 17% of the drainage area was covered by glaciers (Emery et al. 1985). The Chitina River constitutes about one third of the Copper Basin watershed and drains high-altitude snow- and glacier-melt from the surrounding Chugach and Wrangell mountains (Fig. 1). The Chitina River is therefore subject to seasonal freshets during the five-month open-water period from May to September during which approximately 88% of stream flow volume occurs (Emery et al. 1985). Winter freezing and snowfall limits fluvial grain transport to the open-water period.

From the Chitina Glacier terminus to the Copper River confluence, the Chitina River is approximately 188 km long and can be divided into three reaches based on physiographic characteristics. From the nose of the Chitina Glacier to the confluence of the Tana River (~ 80 km; Fig. 1), the Chitina River consists of abundant, tightly braided channels (Fig. 2A) with an average dimensionless slope of 0.004. Channel depths during the sampling transect were commonly up to 2 m. However, note that annual flow can vary substantially and would result in variable channel depths throughout a given year. From the Tana River confluence to the Nizina River confluence (~ 35 km; Fig. 1), the Chitina River forms a single channel (~ 250 m wide) that incises into Pleistocene glacio-lacustrine deposits. This section of the Chitina River comprises almost exclusively transverse bars (Fig. 2B) and has an average dimensionless slope of 0.002 with channel depth during sampling up to 6 m. From the Nizina River confluence to the Copper River confluence (~ 70 km; Fig. 1) the Chitina River channel returns to moderately braided or anastomosing (Fig. 2C) with an average dimensionless slope of 0.002. Transverse bars become more abundant than longitudinal bars after the initial 20 km downstream from the Chitina–Nizina confluence. Approximately 30 km upstream of the Copper River confluence, the Chitina River transforms to a single channel.

The absence of a hydrologic gauging station along the Chitina River makes estimates of mean annual flow challenging. However, a gauging station on the upper Copper River, just downstream from the Chitina–Copper confluence and operating from 1955 to 1985, recorded a mean annual discharge of 1,067 m^3/s and 2846 m^3/s peak annual discharge with an estimated half of the total discharge at the station sourced from the Chitina River (Emery et al. 1985). If this estimation is realistic, then the

Chitina River flows at approximately 530 m^3/s on average and 1420 m^3/s during peak discharge. As discussed above, the Chitina River has three distinct stretches each corresponding to a tributary confluence. Thus, the discharge of the Chitina River itself would decrease up river, on the order of a third for each reach based on size of drainage area of the contributing tributary. Average dimensionless slope over the entire transect is 0.003, which is consistent with sand- and gravel-dominated, bed-load rivers (Blair and McPherson 1994). Discharge and slopes of this magnitude produce sufficiently turbulent flow regimes should allow energetic bed-load transport.

METHODS

The Chitina River provides an excellent natural laboratory to test fluvial modification of glacially induced microtextures because: 1) the bedrock geology is largely devoid of coarse-grained sedimentary strata, reducing the possibility of inherited transport-induced microtextures; 2) gneiss and granite provide abundant first-cycle quartz sand to the glacial system; and 3) the length of the river is sufficiently long to observe overprinting signals under a variety of hydraulic regimes. Samples were collected systematically downstream from the terminal moraine of the Chitina Glacier to the Copper River confluence with sample spacing approximately 1 km for the initial 5 km and 5–7 km thereafter (Fig. 1). In total, 41 samples were recovered along the Chitina River transect. Samples are registered in SESAR (System for Earth Sample Registration) with accompanying micrographs of each sample.

At each sample site, approximately 0.5 kg of sand was collected from surficial material on active longitudinal bars. Transverse bars were used as sampling sites if longitudinal bars were not present at corresponding sampling distances. In the laboratory, sand was sieved for a 250–850 μm fraction and subjected to magnetic mineral separation and hydrogen peroxide treatment to remove heavy minerals and organics, respectively. In order to prevent potential subjectivity and bias in collection of microtextural data, samples were randomly assigned a letter unassociated with collection site prior to processing so that the SEM user was not aware of distance downstream during data collection.

Numerous quartz grains were selected from the 250–850 μm fraction (e.g., large-grain classification of Krinsley and Doornkamp 1973) by hand with a binocular microscope. Utilizing a constrained grain-size population reduces microtexture variability due to grain size (Vos et al. 2014). Selecting medium to coarse sand reduces potential for eolian transport on exposed bars. Randomly selected quartz grains were placed on carbon-taped, aluminum stubs for iridium sputter coating. Microscopy was conducted on a Hitachi S-4300 scanning electron microscope with an accelerating voltage of 15 kV. Working distance was typically 15 mm. All grains demonstrated quartz equivalent peaks using energy-dispersive spectroscopy.

Collection of microtexture data followed guidelines outlined in Mahaney (2002) where individual textures are marked as present or not present. Collecting data in this manner yields occurrence frequency of each microtexture in per grain units. Thus, an occurrence frequency of 20% indicates that 20% of the grains exhibited at least one instance of that specific microtexture. Note that this methodology does not differentiate between a grain exhibiting a single occurrence of a microtexture versus another grain that may exhibit numerous instances of the same microtexture.

In total, 1,076 quartz grains were evaluated over 40 different samples with each sample averaging about 25 grains. The grain size of sample CR-20 was overwhelmingly $<$ 250 μm and did not yield enough grains of 250–850 μm size to analyze, thus is not included in subsequent discussions. An additional 65 grains exceeding 850 μm were evaluated, but only a few grains of this size were present in samples CR-1, CR-5, CR-10, CR-17, and CR-25. This coarser grain-size population mimicked the 250–850 μm microtexture frequencies when $>$ 20 grains in a sample were analyzed. Most samples produced $<$ 20 grains, thus this larger grain size fraction is not presented in this study.

Microtexture identification utilized the procedures by Krinsley and Doornkamp (1973) and Mahaney (2002) with an emphasis not only on shape of microtexture but also on dimensional similarity. Detailed microtexture descriptions are listed in Table 1. This study focuses predominantly on microtextures resulting from fracturing during transport. Those microtextures that reflect surface modification from chemical weathering and precipitation are not presented and were a minor component of observed microtextures.

Depths and velocities of various stretches of the Chitina River were measured in channel centers while rafting. Velocity was measured directly from instantaneous GPS readings and is a measure of boat speed. Velocity readings were variable due to wind friction, local channel variation, and oar propelling; thus, only those taken with minimal wind and no oaring were considered as estimates for surface velocity. Depths were measured off the bow of rafts with a weighted rope. Faster and deeper channels likely inflated depth readings due to increased nonverticality of the rope. Thus, hydrologic parameters calculated with these measurements are at best estimates.

RESULTS

SEM Microtextural Analysis

The results of SEM microtexture analysis are presented in full in Table 2. Examples of the variety of microtextures are displayed in Figure 3. Quartz grains analyzed per sample is variable, ranging from 20 to 52 grains. Based on literature review, Vos et al. (2014) suggested that 20–25 grains per sample is adequate to characterize the microtextural variability. We ran a test using three samples spaced along the transect (CR-2, CR-16, and CR-40; highlighted gray in Table 2) to assess this assumption. Each sample was prepared twice with a similar amount of grains ($n \approx 25$) on two separate subsamples. The chief goal was to compare the microtextural variability at two distinct times of analysis. Some variance in microtextural occurrence was observed between the separate runs; however, when grouped in the genetic categories of sustained shear stress, percussion, and polygenetic the between run variation is $<$ 5% and commonly only 1–2%. Thus, it seems reasonable to assume that the number of grains analyzed per sample captures most of the natural variability in microtextural occurrence in this system.

A summary of key results is presented below and organized into five intervals: 1) sediment from the terminal moraine of the Chitina Glacier is characterized for a baseline of glacial transport; 2) proximal Chitina River samples (CR-2 to CR-9; $\sim$ 17 km reach) upstream of any major glacial or river confluences; 3) samples (CR-10 to CR-21; $\sim$ 63 km reach) from the Barnard Glacier to the Tana River confluence; 4) samples (CR-22 to CR-27; $\sim$ 35 km reach) recovered between confluences of the Tana River and Nizina River that also corresponds to a single channel section of the river; and 5) samples (CR-28 to CR-41; $\sim$ 73 km reach) downstream from the Nizina River confluence to the Chitina–Copper river confluence. Unless otherwise noted, microtextural percentages reported in this section refer to the number of grains exhibiting a particular microtexture.

Glacier Terminus Sample Baseline (CR-1).—Sample CR-1 was collected as a baseline sample of sediment from till of the terminal moraine of Chitina Glacier (Fig. 2D). Grains were angular to subangular with moderate surface relief. The majority of transport-induced microtextures were breakage blocks and conchoidal, linear, and step fractures. Grain-to-grain stylus microtextures (i.e., grooves, gouges, and troughs) occurred on all but four of the grains analyzed, with straight grooves and crescentic

TABLE 2.—*Occurrence frequency of transport induced microtextures.*

									Polygenetic							Sustained shear stress			Percussion		
Sample groupings denoted in text	Sample	Distance from Chitina Glacier terminus (km)	# of grains	Precipitation features	Adhering Particles	Low relief	Medium relief	High relief	Fracture faces	Subparallel linear fractures	Conchoidal fractures	Arc-shaped steps	Linear steps	Mechanically upturned plates	Sharp angular features	Breakage blocks	Curved grooves	Straight grooves	Crescentric gouges	Deep troughs	V-shaped cracks	Edge rounding
Baseline	CR-1	0	52	8	24	11	31	8	22	26	45	15	14	12	1	50	17	26	18	4	2	1
Chitina Glacier to Barnard Glacier	CR-2 (1)	0.14	32	9	23	4	17	9	12	20	29	15	12	9	5	30	18	11	12	6	5	8
	CR-2 (2)	0.14	40	6	13	10	26	4	9	16	23	14	16	10	5	37	11	9	9	4	3	15
	CR-2	0.14	72	15	36	14	43	13	21	36	52	29	28	19	10	67	29	20	21	10	8	23
	CR-3	1.36	23	6	15	5	14	3	8	9	18	14	5	8	1	23	6	11	8	0	5	0
	CR-4	2.52	21	2	10	6	10	3	12	7	14	8	8	5	2	16	11	12	9	1	1	0
	CR-5	3.13	33	0	27	4	20	8	2	13	22	5	6	5	1	31	8	7	3	7	7	3
	CR-6	3.61	22	2	7	2	11	7	6	11	21	6	5	7	2	22	6	12	6	0	3	0
	CR-7	7.64	26	3	15	1	16	8	7	16	11	12	2	8	2	24	6	6	4	4	5	0
	CR-8	12.65	21	11	16	4	11	6	7	7	15	3	3	4	3	20	10	1	4	2	9	1
	CR-9	16.42	28	2	17	4	10	11	2	16	17	11	2	3	3	24	7	3	4	1	15	7
Barnard Glacier to Tana River Confluence	CR-10	21.8	20	1	8	2	6	1	3	3	3	2	1	0	0	6	5	4	1	0	3	1
	CR-11	27.29	25	0	24	6	10	6	4	10	19	1	3	1	1	21	10	12	0	0	15	0
	CR-12	32.81	26	5	22	4	15	3	4	13	13	10	6	6	5	25	12	8	0	0	15	3
	CR-13	37.66	23	7	19	3	8	10	3	10	17	10	6	7	3	21	12	5	4	0	17	1
	CR-14	43.74	25	1	20	3	10	8	5	9	9	9	5	3	0	19	10	8	1	1	9	0
	CR-15	49.89	20	1	16	1	6	12	3	7	17	7	2	6	4	19	7	2	2	0	18	0
	CR-16(1)	55.23	25	1	20	2	15	6	7	8	11	14	5	8	3	20	12	9	1	2	8	4
	CR-16(2)	55.23	22	0	13	6	5	11	5	5	10	8	5	5	4	13	11	5	1	1	6	2
	CR-16	55.23	47	1	33	8	20	17	12	13	21	22	10	13	7	33	23	14	2	3	14	6
	CR-17	59.8	22	3	16	1	9	10	3	13	14	5	0	3	4	20	9	3	1	3	12	4
	CR-18	65.35	25	2	18	0	10	13	2	11	15	4	1	9	0	25	12	11	5	1	15	0
	CR-19	70.47	22	7	13	6	8	7	8	11	3	6	2	7	6	19	14	9	3	0	13	1
	CR-20	73.99	sample did not yield enough 250–850 μm to be included in analysis																			
	CR-21	80.01	21	0	14	2	7	10	4	11	9	7	6	5	3	20	17	4	2	0	10	1

gouges most common (Table 1). Fractures that indicate grain-to-grain impacts, v-shaped cracks, and edge rounding textures occurred on only three grains.

Proximal Chitina River Samples (CR-2 to CR-9).—Samples CR-2 to CR-9 were collected progressively downstream from the Chitina Glacier terminus to a point just upstream of influence from the Barnard Glacier (Fig. 1). The subangular to subrounded grains exhibited predominantly medium relief. Grains displaying stylus features include curved grooves ($\bar{X}$ = 33%, range = 23–52%), straight grooves ($\bar{X}$ = 31%, range = 5–57%), crescentic gouges ($\bar{X}$ = 24%, range = 9–43%), and deep troughs ($\bar{X}$ = 9%, range = 0–21%). However, occurrence frequency of grain-to-grain stylus microtextures decreases downstream from 21–31% of total microtextures within 4 km of the terminal moraine to as low as 13% of the microtextures at 16 km downstream. Grains exhibiting grain-to-grain impact features include v-shaped cracks ($\bar{X}$ = 23%, range = 5–54%) and edge rounding ($\bar{X}$ = 9%, range = 0–32%). Grain-to-grain impact microtextures increase downstream from < 8% over the first 4 km up to 19% at 16 km downstream. All grains display some form of polygenetic fracturing, including breakage blocks, mechanically upturned plates, and conchoidal, step, and linear fractures.

Barnard Glacier to Tana River Confluence (CR-10 to CR-21).—Quartz grain samples collected downstream from the Barnard Glacier (CR-10) to the Tana River confluence (CR-21; Fig.1) are subrounded to rounded with medium to high relief. Microtextures such as breakage blocks and step, conchoidal, and linear fractures are the most prevalent. Most grains exhibited stylus microtextures and include curved grooves ($\bar{X}$ = 47%, range = 25–81%), straight grooves ($\bar{X}$ = 28%, range = 10–48%), crescentic gouges ($\bar{X}$ = 8%, range = 0–20%), and deep troughs ($\bar{X}$ = 3%, range = 0–14%). Stylus microtextures increased in occurrence frequency at the Barnard Glacier (up to ~ 31%) approaching the baseline terminal-moraine values. Yet downstream of the Hawkins Glacier, the stylus microtextures range as low as 12%. Approximately 72% of the grains demonstrate grain-to-grain impact microtextures and include v-shaped cracks ($\bar{X}$ = 53%, range = 15–90%) and edge rounding ($\bar{X}$ = 6%, range = 0–18%).

TABLE 2.—*Continued*.

									Polygenetic							Sustained shear stress				Percussion	
Sample groupings denoted in text	Sample	Distance from Chitina Glacier terminus (km)	# of grains	Precipitation features	Adhering Particles	Low relief	Medium relief	High relief	Fracture faces	Subparallel linear fractures	Conchoidal fractures	Arc-shaped steps	Linear steps	Mechanically upturned plates	Sharp angular features	Breakage blocks	Curved grooves	Straight grooves	Crescentric gouges	Deep troughs	V-shaped cracks	Edge rounding
Tana River Confluence to Nizina River Confluence	CR-22	85.8	23	0	15	4	8	9	5	10	9	13	1	3	2	19	13	6	2	1	13	0
	CR-23	92.15	29	0	22	4	16	9	4	9	17	19	7	6	0	28	14	9	3	2	16	2
	CR-24	98.24	20	0	18	1	12	6	4	5	9	4	8	2	2	19	10	2	3	1	19	1
	CR-25	105.1	29	0	21	2	14	11	8	20	22	8	6	1	2	29	6	6	0	0	18	0
	CR-26	110.33	22	1	17	2	8	10	7	19	11	2	3	3	5	19	5	2	1	1	18	9
	CR-27	115.48	25	0	24	2	13	8	3	17	21	7	5	2	0	25	6	1	0	0	23	7
Nizina River Confluence to the Copper River	CR-28	120.85	21	0	17	3	8	9	4	11	17	9	8	1	2	21	4	1	2	0	15	0
	CR-29	125.18	28	0	28	7	9	7	4	9	20	6	8	2	0	28	7	1	0	0	25	7
	CR-30	130.77	22	2	19	4	7	10	8	11	11	4	7	3	4	21	6	4	0	0	10	4
	CR-31	136.42	21	0	21	0	14	7	2	8	21	6	3	1	0	21	4	3	0	1	16	3
	CR-32	139.64	22	0	21	2	8	9	3	12	15	3	11	4	6	22	2	3	1	2	15	3
	CR-33	143.69	23	1	18	1	9	12	6	8	10	8	5	5	2	19	11	3	3	1	15	4
	CR-34	148.91	21	0	21	1	5	15	3	10	16	4	6	2	1	21	6	0	0	3	19	0
	CR-35	154.37	21	0	20	2	14	3	3	6	17	6	9	1	0	21	4	2	0	2	15	1
	CR-36	160.74	34	1	25	5	18	10	11	11	19	11	4	2	2	30	11	2	0	2	27	7
	CR-37	166.17	21	0	21	0	10	9	2	14	20	3	9	0	3	21	7	2	0	0	21	4
	CR-38	171.45	26	0	19	0	13	7	5	15	19	5	8	0	0	26	7	2	0	0	23	11
	CR-39	176.91	26	0	26	0	8	13	7	12	14	5	3	0	0	26	7	2	0	0	23	12
	CR-40(1)	181.96	25	0	24	2	11	12	5	10	15	12	8	4	1	24	8	3	0	1	24	4
	CR-40(2)	181.96	21	5	12	2	13	6	0	16	17	3	8	4	0	11	4	1	2	1	21	7
	CR-40	181.96	46	5	36	4	24	18	5	26	32	15	16	8	1	35	12	4	2	2	45	11
	CR-41	188.2	22	0	19	0	13	7	4	12	16	0	7	1	5	22	2	4	0	0	20	13

Shaded cells are duplicate runs of same locality for assessment of sample-size sensitivity.
(1) first run of sample in sensitivity study. (2) second run of sample in sensitivity study.

Tana River to Nizina River Confluence (CR-22 to CR-27).— Samples collected downstream from the Tana River confluence (CR-22) and upstream of the Nizina River confluence (CR-27; Fig. 1) are subrounded and commonly exhibit medium surface relief. Grains exhibiting v-shaped cracks ($\bar{X}$ = 74%, range = 55–95%) and edge rounding ($\bar{X}$ = 14%, range = 0–41%) generally are greater than samples collected upstream. Grains with stylus microtextures include grooves ($\bar{X}$ = 37%, range = 21–57%), straight grooves ($\bar{X}$ = 17%, range = 4–31%), crescentic gouges ($\bar{X}$ = 6%, range = 0–15%), and deep troughs ($\bar{X}$ = 4%, range = 0–7%). Within the interval, substantial downstream trends occur from CR-22 to CR-27 with increasing abundance of v-shaped cracks and edge rounding, but decreasing abundance of stylus microtextures.

Nizina River Confluence to Copper River Confluence (CR-28 to CR-41).—Quartz grains analyzed between the Nizina and Copper River confluences (~ 65 km; Fig. 1) are subrounded with predominantly medium relief. Grains exhibiting stylus microtextures including curved grooves ($\bar{X}$ = 25%, range = 9–48%), straight grooves ($\bar{X}$ = 10%, range = 0–18%), crescentic gouges ($\bar{X}$ = 2%, range = 0–13%), and deep troughs ($\bar{X}$ = 4%, range = 0–14%) is lower than upstream stretches of river. Conversely, grains exhibiting v-shaped cracks ($\bar{X}$ = 80%, range = 45–100%) and edge rounding ($\bar{X}$ = 21%, range = 0–59%) is typically greater than samples collected upstream. Within the interval, grains exhibiting v-shaped cracks and edge-rounding microtextures increase substantially downstream.

Transport-Induced Microtextural Suites

The Chitina River dataset displays a variety of transport-induced microtextures. Grains have experienced both glacial transport under sustained shear stress and fluvial transport with saltation and traction. These two transport styles produce different microtextures; thus the data have been grouped into microtexture suites reflecting transport styles, similarly to other studies (Campbell and Thompson 1991; Sweet and Soreghan 2010). Henceforth, the data are compared using sustained shear stress, percussion, and polygenetic microtextural groups. Percentages reported in this section represent the number of microtextures in one of the three suites as a percentage of total microtexture observations taken from Table 2.

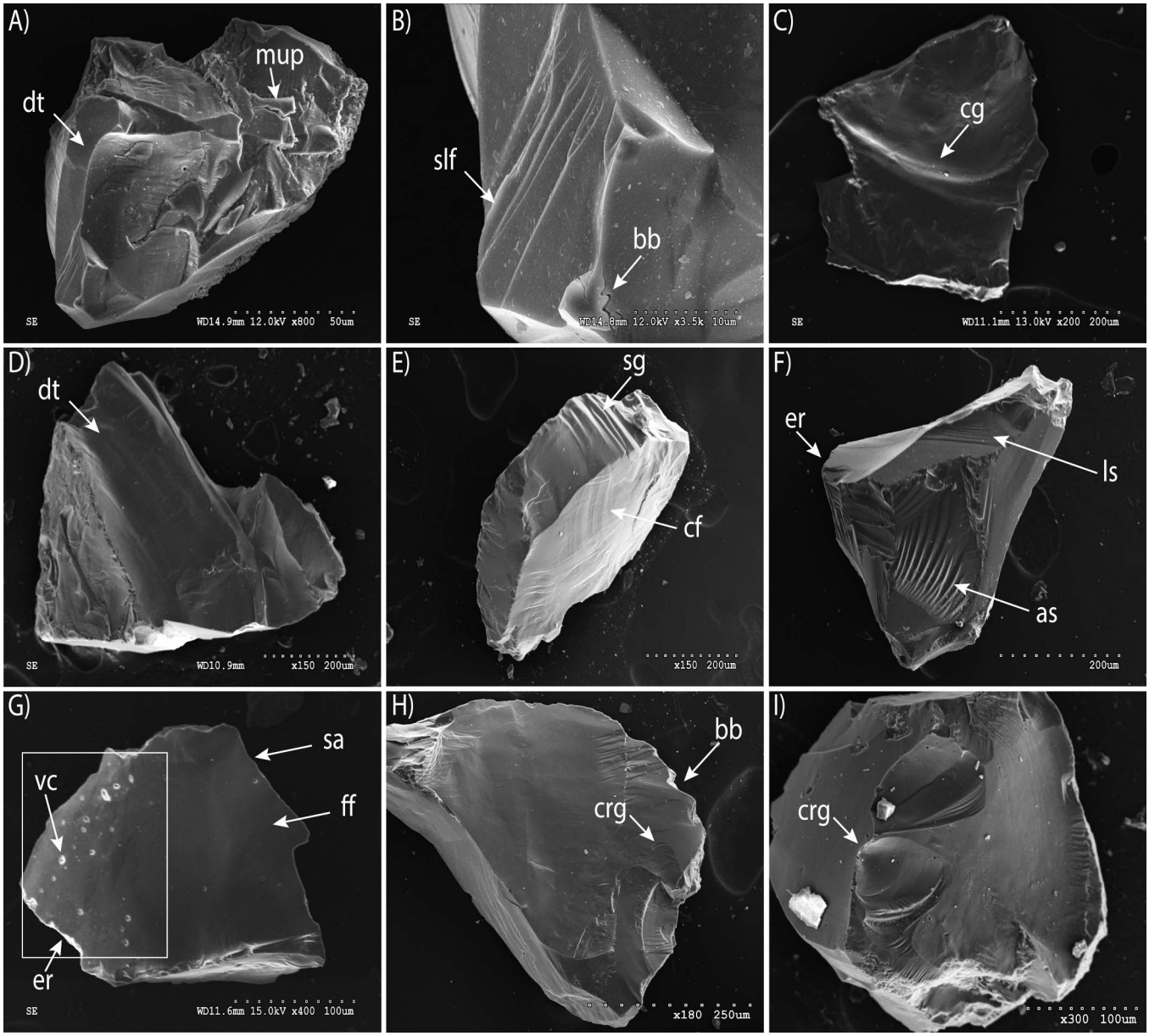

FIG. 3.—SEM micrographs demonstrating the variety of transport-induced microtextures categorized and collected in Table 2. See Table 1 for corresponding dimensions of features. Most of the grains in this figure record multiple microtextures that are not labeled. Microtextures that are labeled indicate representative examples. **A)** Angular quartz grain displaying high relief, mechanically upturned plate (mup), and deep trough (dt). The deep trough is estimated at 10–15 μm deep. **B)** Angular quartz grain with subparallel linear fractures (slf). Microtextures are differentiated from linear steps by spacing < 5 μm. Note the incompletely fractured block, or breakage block (bb), on the bottom edge of the grain. **C)** Curved groove (cg) across grain surface. Depth of groove approaches 10 μm. **D)** Irregular quartz grain with deep trough (dt) at least 30 μm deep. **E)** Angular quartz grain displaying straight grooves (sg; $\sim$ 15 μm deep) and conchoidal fracturing (cf). **F)** Linear steps (ls; 5–20 μm spacing) and arc-shaped steps (as; 10–20 μm deep with similar spacing). Many of the edges demonstrate rounding (er). **G)** Semi-angular quartz grain with v-shaped cracks (vc) housed within white box, sharp angular features (sa), and fracture faces (ff). The bottom left grain edge demonstrates edge rounding (er). **H)** Whole-grain view demonstrating numerous locations on grain edges where a block has broken off. Compare these breakage blocks (bb) with the example in Part B that is an incompletely broken block. Crescentic gouge (crg) also present on surface and is $\sim$ 20 μm deep in the center. **I)** Crescentic gouge (crg) on grain surface. Note the initiation point of the crescentic gouge (white arrow) and the propagation away from that point. Gouge is $\sim$ 10 μm deep in the center.

Downstream Trends of the Microtexture Suites

A reciprocal relationship between percussion and sustained-shear-stress microtextures is observed over the entire length of the Chitina River. Polygenetic microtextures demonstrate no discernible trend with distance downstream (Fig. 4). Sustained-shear-stress microtextures are variable downstream ($\sigma = 7\%$) but a modest negative correlation ($R^2 = 0.58$) exists. Percussion microtextures positively correlate ($R^2 = 0.69$) to distance downstream with similar variability ($\sigma = 8\%$). Polygenetic microtextures do not correlate to distance downstream and are the most abundant (range $= 56$–77%) with the least variability ($\sigma = 5\%$; Fig. 4).

Various short-distance trends also occur in the data. Grains over the first $\sim$ 17 km (CR-2 to CR-9) demonstrate a decrease in occurrence frequency of sustained-shear-stress microtextures, whereas percussion microtextures

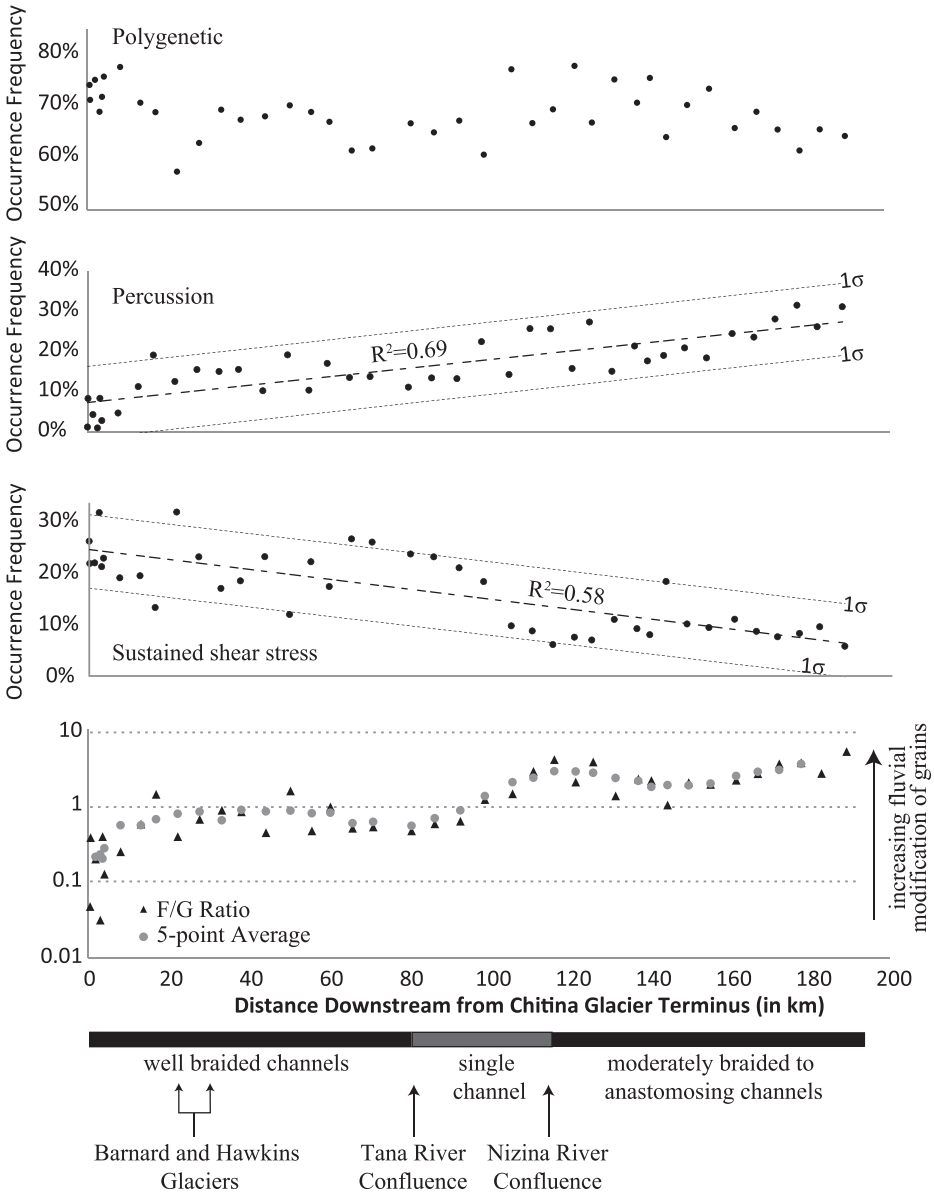

FIG. 4.—Various microtextural abundances plotted versus distance downstream. The percentages of polygenetic, percussion, and sustained-shear-stress microtexture suites sum to 100 in each sample. The F/G ratio (black triangles) is the occurrence frequency of percussion microtextures divided by the occurrence frequency of sustained-shear-stress microtextures. Notable physiographic components of the Chitina River watershed are shown at the bottom of the figure. Specific trends discussed in the manuscript are tied to the distance scale at the bottom of the figure.

increase. Polygenetic microtextures show very little variation and no correlation to distance downstream. These relationships indicate that percussion-induced microtextures increase at the expense of sustained-shear-stress microtextures. Indeed, by sample CR-9, percussion microtextures exceed sustained-shear-stress microtextures by 6%.

From ~ 80 to 115 km distance downstream (CR-22 to CR-27), occurrence frequency of sustained-shear-stress and percussion microtextures decreases and increases downstream, respectively. As with previous intervals, polygenetic microtextures poorly correlate to distance downstream. At ~ 100 km, the occurrence frequency of sustained-shear-stress microtextures decreases in magnitude below the occurrence frequency of percussion microtextures (Fig. 4).

The final segment of downstream transport, from ~ 115–188 km (CR-28 to CR-41) sustained-shear-stress microtextures continue to slightly decrease, but not substantially, and remain predominantly below percussion microtextural percentages. With the exception of CR-33 (18%), sustained-shear-stress microtextures are near or below 10%. In contrast, occurrence frequency of percussion microtextures increases downstream from ~ 15% to 30% and are some of the highest values of this microtextural group.

DISCUSSION

Ratio of Fluvially to Glacially Induced Microtextures

Sustained-shear-stress microtextures are most commonly reflective of glacial transport (Table 1). As discussed earlier, highly viscous debris flows and structural shear zones can impart stylus microtextures (Mahaney 2002). We infer that straight and curved grooves, deep troughs, and crescentic gouges are predominantly glacially induced microtextures in this study because any debris flows or structural shear zones that intersect the Chitina Glacier would provide volumetrically minimal material when compared to glacial erosion. In this study, percussion microtextures must reflect aqueous saltation and traction from transport along the Chitina River or its tributaries plus any subglacial fluvial transport. Eolian modification of grains is considered minor, if at all, because: 1) grain size analyzed is quite coarse (250–850 μm) for eolian transport; 2) lengths of

the bar tops limit the distance of potential eolian transport; and 3) frozen ground and snow cover would hinder eolian entrainment during the low-discharge winter months. Thus, the ratio of percussion microtextures to sustained-shear-stress microtextures versus distance downstream should reflect the relative abundance of fluvially to glacially modified grains.

The ratio of fluvially to glacially induced microtexture (F/G ratio) generally increases downstream with only localized river stretches decreasing (Fig. 4). A five-point running average of the ratio was calculated to smooth the data and potentially reveal inflection points in the slope of the ratio. The F/G ratio increases relatively steadily over the first $\sim$ 17 km of transport, and then demonstrates a slight decrease until $\sim$ 80 km (Fig. 4). The $\sim$ 17 km and $\sim$ 80 km distances correspond to important geomorphic variations in the watershed. From the Chitina Glacier terminus to $\sim$ 17 km, the Chitina River maintains tightly braided channels, no substantial tributary, and limited Pleistocene deposits for recycling (Richter et al. 2006); thus the predominant influence on grain surface modification is transport from the Chitina River. However, from $\sim$ 17 to $\sim$ 33 km downstream, the Barnard and Hawkins glaciers are intersected by the Chitina River (Fig. 1). Grains sampled (CR-10 to CR-12) in this stretch of river exhibit an increase in occurrence frequency of glacially induced microtextures corresponding to a decrease in the F/G ratio (Fig. 4). A reasonable cause for this change is an influx of grains from the Barnard and Hawkins glaciers. The glaciers supply sediment to the Chitina River which has experienced predominantly glacial transport with little to no fluvial transport. Thus, the microtextural characteristics of the grains likely resemble sediment from the Chitina Glacier terminal moraine (CR-1). This influx of new material with a predominant glacial transport history should decrease the F/G ratio.

Downstream from the Barnard and Hawkins glaciers and upstream of the Tana River confluence, the F/G ratio continues to decrease slightly. In theory, grains along this stretch of river should be modified by fluvial transport such that the F/G ratio increases. The reason for this discrepancy between theory and observation is not clear, but one contributing factor may be recycling of Pleistocene glacial drift which borders the active floodplain of the Chitina River from the Hawkins Glacier to the Copper River confluence (Richter et al. 2006). Assuming that the microtextural character of the glacial drift is similar to the CR-1 sample, recycling quartz grains from surrounding Pleistocene deposits may produce enough glacial grains to counteract fluvial surface modification, resulting in a steady F/G ratio. A potential issue with recycling of Pleistocene drift is the overall abundance of freshly fractured surfaces and paucity of weathered and/or precipitation features on the quartz grains often observed in microtextural studies of glacial deposits of similar age (e.g., Mahaney and Kalm 2002; Kirshner and Anderson 2011).

Alternatively, the decreasing F/G ratio trend along this stretch of river (CR-13 to CR-21) may be related to flow characteristics. River morphology here is extensively braided resulting in the shallowest channel depths (commonly $<$ 1 m) observed along the Chitina River. The stretch also had the highest range of instantaneous GPS estimates of flow velocity (2.5 to 4 m/s) at the water surface. For comparison, estimates for flow velocity (2 to 3 m/s) at the water surface and channel depths (1 to 3 m) were commonly slower and deeper, respectively, for the stretch of river upstream of the Barnard Glacier. Shallower channels should result in lower shear values at the flow boundary which may hinder grain entrainment. However, once a grain is entrained, the faster flow velocities should have resulted in higher degree of turbulence and potentially longer periods of suspension during saltation. Taken together, these flow characteristics may have resulted in fewer chances to impart percussion microtextures. Longer suspension may also have been amplified if the Hawkins and Bernard glaciers increased suspended silt and associated water turbidity. A clear interpretation is difficult, but it seems probable that recycling of Pleistocene glacial drift and/or flow parameters had some control in suppressing the F/G ratio along this river stretch.

After the Tana River confluence, the Chitina River forms a single-channel river. From the Tana River to the Nizina River confluence ($\sim$ 81 to 115 km), the F/G ratio increases by nearly an order of magnitude (Fig. 4). At least two factors potentially contribute to this increase. First, sediment supplied by the Tana River has experienced $\sim$ 50 km of transport after liberation from the Tana Glacier (Fig. 1). This distance of fluvial transport should have imparted a significant component of fluvially induced microtextures atop glacial microtextures. However, the F/G ratio continues to increase steadily after the confluence, suggesting additional controls. The second factor seems intrinsic to this particular stretch of river. Here, estimates of flow velocity (1.5 to 2 m/s) at the water surface are lower than upstream stretches which may have resulted in shorter saltation distances. The Chitina River coalesces into a single channel along this stretch resulting in the deepest channel measurements (up to 6 m). Flow depths of this magnitude should result in the highest shear values at the flow boundary. The predominantly cobble- and boulder-armored transverse bars along this stretch are consistent with high shear stress values. Taken together, grains transported along this stretch of river were likely continuously undergoing saltation with relatively short distances between impacts, which ultimately increases the chances to impart percussion microtextures. Thus, in absence of a glacial source except as background recycling of Pleistocene glacial drift, progressive downstream fluvial transport resulted in a steady and substantial increase in the F/G ratio along this stretch of river.

The Chitina River transforms back to a weakly braided to anastomosing system after the Nizina River confluence (Figs. 1, 2C). This morphologic change also coincides with an increase in sediment delivery and discharge from the Nizina River. Even with increasing discharge and sediment supply, the F/G ratio decreases by nearly a factor of 2 after the Nizina River confluence (Fig. 4). The Nizina River should have supplied grains with up to 60 km of percussion related transport (Fig. 1) and suppressed the ratio. However, approximately 20 km upstream of the Nizina River confluence, the Kennicott Glacier supplies sediment to the Nizina River. Thus, if these grains exhibit microtextural character similar to that of grains from the Chitina Glacier terminal moraine (CR-1), then the addition of glacially induced microtextures should result in a decrease of the F/G ratio. Occurrence frequency of sustained-shear-stress microtextures do generally increase just downstream of the Nizina River confluence. Approximately 50 km downstream from the Nizina River confluence, the F/G ratio begins to substantially increase, so that by the end of the Chitina River the ratio is at three to four. The progressive increase is likely attributable to increasing distance of saltation and traction transport.

Application to Ancient Proglacial Systems

Currently, coarse-grained fluvial depositional models are categorized as glacial or nonglacial largely on the basis of extensive and abundant flooding episodes during melting periods (e.g., Maizels 1993, 1997; Marren 2002). However, flooding may result from natural variation in seasonal flow from means other than glacial melt. Microtextural analysis of quartz grains from ancient strata could be a proxy for glacial influence on ancient fluvial strata through the presence of glacially induced microtextures. Thus, utilizing quartz grain microtextures from ancient braided rivers can significantly augment current facies models.

In the Chitina River, the F/G ratio appears to be sensitive enough to grossly predict major tributary confluences and/or valley-glacier intersections (Fig. 4). Potentially, the F/G ratio may record similar physiographic features in other modern proglacial systems. If so, then applicability of the ratio to ancient systems might help in paleogeographic reconstructions.

CONCLUSION

SEM analysis of quartz grains from the Chitina River, SE Alaska, demonstrates that glacially induced microtextures decrease with distance

of fluvial transport, fluvially induced microtextures increase with downstream fluvial transport, and polygenetic microtextures show no relationship to distance of transport. Glacially induced microtextures (i.e., straight and curved grooves, deep troughs, and crescentic gouges) are observed in all samples collected from the Chitina River. Results of this study support the survival of glacially induced microtextures on grains for at least ~ 188 km of fluvial transport, if hydrologic and physiographic conditions are/were similar to the Chitina River. At the end of the sampling transect, it is unclear if the dominant source of grains exhibiting glacially induced microtextures is still the Chitina Glacier because multiple glacial origins are possible along the entire stretch of river. However, the persistent presence of sustained-shear-stress microtextures indicates that if this style of microtextures is observed in ancient fluvial strata, then a reasonable interpretation is proglacial. These data support the argument that this tool can be used as a proxy to determine the presence of ice in ancient systems that are lacking a clear sedimentologic signature.

Fluvial transport modifies the surface of glacially derived grains progressively downstream. The F/G ratio and occurrence frequency of sustained-shear-stress and percussion microtextures demonstrate either positive or negative correlation to distance downstream. The F/G ratio appears to grossly record physiographic changes in the Chitina River. The most direct response is an increase in the F/G ratio at major river tributaries. Additionally, the F/G ratio decreases as valley glaciers are intersected by the Chitina River. These results should be corroborated with other modern proglacial rivers to assess the potential for developing predictable relationships between downstream distance of transport and microtextural abundances.

ACKNOWLEDGMENTS

This study was partially funded by National Science Foundation grant EAR-1324818 (to Sweet) and American Association of Petroleum Geologists Southwest Section student grant (to Brannan). The opinions, findings, conclusions, or recommendations expressed in the manuscript are the authors' and do not necessarily reflect the views of the funding agencies. Peer review by N. Immonen, an anonymous reviewer, and associate editor B. Ward improved the manuscript message to maximize impact. Scanning electron microscopy utilized equipment in the Texas Tech University College of Arts & Sciences Microscopy obtained through National Science Foundation Grant MRI-04-511. We thank B. Zhao for expertise in electron microbeam equipment. Lastly, we thank the most excellent staff at Copper Oar, including guides D. Meck and E. Baade, in McCarthy, Alaska, for running a safe and well organized sampling trip to a new location.

REFERENCES

Alley, R.B., Cuffey, K.M., Evenson, E.B., Strasser, J.C., Lawson, D.E., and Larson, G.J., 1997, How glaciers entrain and transport basal sediment: physical constraints: Quaternary Science Reviews, v. 16, p. 1017–1038.

Al-Saleh, S., and Khalaf, F.I., 1982, Surface textures of quartz grains from various recent sedimentary environments in Kuwait: Journal of Sedimentary Petrology, v. 52, p. 215–225.

Biederman, E.W., 1962, Distinction of shoreline environments in New Jersey: Journal of Sedimentary Petrology, v. 32, p. 181–200.

Blair, T.C., and McPherson, J.G., 1994, Alluvial fans and their natural distinction from rivers based on morphology, hydraulic processes, sedimentary processes, and facies assemblages: Journal of Sedimentary Research, v. 64, p. 450–489.

Boothroyd, J.C., and Ashley, G.M., 1975, Process, bar morphology, and sedimentary structures on braided outwash fans, northeastern Gulf of Alaska, *in* Jopling, A.V., and McDonald, B.C., eds., Glacio-Fluvial and Glaciolacustrine Sedimentation: Society of Economic Paleontologists and Mineralogists, Special Paper 23, p. 193–222.

Boothroyd, J.C., and Nummendal, D., 1978, Proglacial braided outwash: a model for humid alluvial-fan deposits, *in* Miall, A.D., ed., Fluvial Sedimentology: Canadian Society of Petroleum Geologists, Memoir 5, p. 641–668.

Brown, J.E., 1973, Depositional histories of sand grains from surface textures: Nature, v. 242, p. 396–398.

Campbell, S., and Thompson, I.C., 1991, The palaeoenvironmental history of Late Pleistocene deposits at Moel Tryfan, North Wales: evidence from Scanning Electron Microscopy (SEM): Proceedings of the Geologists' Association, v. 102, p. 123–134.

Cuffey, K.M., Conway, H., Gades, A.M., Hallet, B., Lorrain, R., Severinghaus, J.P., Steig, E.J., Vaugh, B., and White, J.W.C., 2000, Entrainment at cold glacier beds: Geology, v. 28, p. 351–354.

Curry, A.M., Porter, P.R., Irvine-Fynn, T.D.L., Rees, G., Sands, T.B., and Puttick, J., 2009, Quantitative particle size, microtextural and outline shape analyses of glacigenic sediment reworked by paraglacial debris flows: Earth Surface Processes and Landforms, v. 34, p. 48–62.

D'Orsay A.M., and van de Poll, H.W., 1985, Quartz grains surface textures: evidence for middle Carboniferous glacial sediment input to the Parrsboro Formation of Nova Scotia: Geology, v. 13, p. 285–287.

Emery, P.A., Jones, S.H., and Glass, R.L., 1985, Water resources of the Copper River Basin, Alaska: U.S. Geological Survey, Hydrologic Investigations Atlas HA-686, 3 sheets.

Fischer, U.H., and Clarke, G.K.C., 1997, Stick–slip sliding behaviour at the base of a glacier: Annals of Glaciology, v. 24, p. 390–396.

Helland, P.E., and Diffendal, R.F., Jr., 1993, Probable glacial climatic conditions in source areas during deposition of the Ash Hollow Formation, Ogallala Group (late Tertiary), of western Nebraska: American Journal of Science, v. 293, p. 744–757.

Hossain, H.M.Z., Tarek, M., Armstrong-Altrin, J.S., Monir, M.M.U., Ahmed, M.T., Ahmed, S.I., and Hernandez-Coronado, C.J.J., 2014, Microtextures of detrital sand grains from the Cox's Bazar beach, Bangladesh: implications for provenance and depositional environment: Carpathian Journal of Earth and Environmental Sciences, v. 9, p. 187–197.

Immonen, N., Strand, K., Huusko, A., and Lunkka, J.P., 2014, Imprint of late Pleistocene continental processes visible in ice-rafted grains from the central Arctic Ocean: Quaternary Science Reviews, v. 92, p. 133–139.

Jackson, G., 1996, Stratigraphy and paleohydraulic analysis of glacial and meltwater sediments in the Mesa del Caballo area, Sierra de Santo Domingo, Venezuelan Andes, *in* Mahaney, W.C., and Kalm, V., eds., Field Guide for the International Conference on Quaternary Glaciation and Paleoclimate in the Andes Mountains: Toronto, Ontario, Quaternary Surveys, p. 57–66.

Johnson, W.H., and Hansel, A.K., 1999, Wisconsin Episode glacial landscape of central Illinois: a product of subglacial deformation processes?, *in* Mickelson, D.M., and Attig, J.W., eds., Glacial Processes Past and Present: Geological Society of America, Special Paper 337, p. 121–135.

Keiser, L.J., Soreghan, G.S., and Kowalewski, M., 2015, Use of quartz microtextural analysis to assess possible proglacial deposition for the Pennsylvanian–Permian Cutler Formation (Colorado, U.S.A.): Journal of Sedimentary Research, v. 85, p. 1310–1322.

Kirshner, A.E., and Anderson, J.B., 2011, Cenozoic glacial history of the northern Antarctic Peninsula: a micromorphological investigation of quartz sand grains, *in* Anderson, J.B., and Wellner, J.S., eds., Tectonic, Climatic, and Cryospheric Evolution of the Antarctic Peninsula: American Geophysical Union, Special Publication 63, p. 153–165.

Krinsley, D.H., and Donahue, J., 1968, Environmental interpretation of sand grain surface textures by electron microscopy: Geological Society of America, Bulletin, v. 79, p. 743–748.

Krinsley, D.H., and Doornkamp, J.C., 1973, Atlas of Sand Grain Surface Textures: Cambridge, U.K., Cambridge University Press, 91p.

Krinsley, D., and Takahashi, T., 1962, Applications of electron microscopy to geology: New York Academy of Science, Transactions, v. 25, p. 3–22.

MacKevett, E.M., 1970, Geology of the McCarthy B-4 Quadrangle, Alaska: U.S. Geological Survey, Bulletin 1333, 31 p.

Mahaney, W.C., 2002, Atlas of Sand Grain Surface Textures and Applications: Oxford, U.K., Oxford University Press, 237 p.

Mahaney, W.C., and Andres, W., 1991, Glacially crushed quartz grains in loess as indicators of long-distance transport from major European ice centers during the Pleistocene: Boreas, v. 20, p. 231–239.

Mahaney, W.C., and Andres, W., 1996, Scanning electron microscopy of quartz sand from the north-central Saharan desert of Algeria: Zeitschrift für Geomorphologie, Supplement B, v. 103, p. 179–192.

Mahaney, W.C., and Dohm, J.M., 2011, The 2011 Japanese 9.0 magnitude earthquake: test of a kinetic energy wave model using coastal configuration and offshore gradient of Earth and beyond: Sedimentary Geology, v. 239, p. 80–86.

Mahaney, W.C., and Kalm, V., 1995, Scanning electron microscopy of Pleistocene tills in Estonia: Boreas, v. 24, p. 13–29.

Mahaney, W.C., and Kalm, V., 2000, Comparative SEM study of oriented till blocks, glacial grains and Devonian sands in Estonia and Latvia: Boreas, v. 29, p. 35–51.

Mahaney, W.C., Vortsich, W., and Julig, P.J., 1988, Relative differences between glacially crushed quartz transported by mountain and continental ice, some examples from North America and East Africa: American Journal of Science, v. 288, p. 810–826.

Mahaney, W.C., Claridge, G., and Campbell, I., 1996, Microtextures on quartz grains in tills from Antarctica: Palaeogeography, Palaeoclimatology, Palaeoecology, v. 121, p. 98–103.

Mahaney, W.C., Stewart, A., and Kalm, V., 2001a, Quantification of SEM microtextures useful in sedimentary environmental discrimination: Boreas, v. 30, p. 165–171.

Mahaney, W.C., Dohm, J., Baker, V.R., Newsom, H., Malloch, D., Hancok, R.G.V., Campbell, I., Sheppard, D., and Milner, M.W., 2001b, Morphogenesis of Antarctic paleosols: Martian analog: Icarus, v. 154, p. 113–130.

Mahaney, W.C., Russell, S.E., Milner, M.W., Kalm, V., Bezada, M., Hancock, R.G.V., and Beukens, R., 2001c, Paleopedology of middle Wisconsin/Weishselian paleosols in the Mérida Andes, Venezuela: Geoderma, v. 104, p. 215–237.

Maizels, J., 1993, Lithofacies variations within sandur deposits: the role of runoff regime, flow dynamics and sediment supply characteristics: Sedimentary Geology, v. 85, p. 299–325.

Maizels, J., 1997, Jökulhlaup deposits in proglacial areas: Quaternary Science Reviews, v. 16, p. 793–819.

MacKevett, E.M., 1978, Geologic map of the McCarthy Quadrangle, Alaska: U.S. Geological Survey, Miscellaneous Investigation Series, Map I-1032, 1 sheet, scale 1:250000.

Malhame, P., and Hesse, R., 2015, Quartz arenites of the Cambro-Ordovician Kamouraska Formation, Quebec Appalachians, Canada: II. Eolian sands in deep-sea sedimentary gravity-flow deposits: Canadian Journal of Earth Sciences, v. 52, p. 261–277.

Margolis, S., 1968, Electron microscopy of chemical solution and mechanical abrasion features on quartz sand grains: Sedimentary Geology, v. 2, p. 243–256.

Marren, P.M., 2002, Glacier margin fluctuations, Skaftafellsjökull, Iceland: implications for sandur evolution: Boreas, v. 31, p. 75–81.

Mazzullo, J., 1987, Origin shapes in the St. Peter Sandstone: determination by Fourier shape analysis and scanning electron microscopy, *in* Marshall, J.R., ed., Clastic Particles: Reinhold, New York, Van Nostran, p. 302–313.

Mazzullo, J., and Ritter, C., 1991, Influence of sediment source on the shapes and surface textures of glacial quartz sand grains: Geology, v. 19, p. 384–388.

Miall, A.D., 1978, Lithofacies types and vertical profile models in braided river deposits: a summary, *in* Miall, A.D., ed., Fluvial Sedimentology: Canadian Society of Petroleum Geologists, Memoir 5, p. 597–604.

Nokleberg, W.J., Jones, D.L., and Silberling, N.J., 1985, Origin and tectonic evolution of the Maclaren and Wrangellia terranes, eastern Alaska Range, Alaska: Geological Society of America, Bulletin, v. 96, p. 1251–1270.

Nokleberg, W.J., Plafker, G., and Wilson, F.H., 1994, Geology of south-central Alaska, *in* Plafker, G., and Berg, H.C., eds., The Geology of Alaska: Geological Society of America, The Geology of North America v. G-1, p. 311–364.

Porter, J.J., 1962, Electron microscopy of sand surface features: Journal of Sedimentary Petrology, v. 32, p. 124–135.

Richter, D.H., Preller, C.C., Labay, K.A., and Shew, N.B., 2006, Geologic Map of the Wrangell–Saint Elias National Park and Preserve, Alaska: U.S. Geological Survey, Scientific Investigations Map 2877.

Strand, K., Passchier, S., and Näsi, J., 2003, Implications of quartz grain microtextures for onset Eocene/Oligocene glaciation in Prydz Bay, ODP Site 1166, Antarctica: Palaeogeography, Palaeoclimatology, Palaeoecology, v. 198, p. 101–111.

Sweet, D.E., and Soreghan, G.S., 2008, Polygonal cracking in coarse clastics records cold temperatures in the equatorial Fountain Formation (Pennsylvanian–Permian, Colorado): Palaeogeography, Palaeoclimatology, Palaeoecology, v. 268, p. 193–204.

Sweet, D.E., and Soreghan, G.S., 2010, Application of quartz sand microtextural analysis to infer cold-climate weathering for the equatorial Fountain Formation (Pennsylvanian–Permian, Colorado, USA): Journal of Sedimentary Research, v. 80, p. 666–677.

Trop, J.M., Ridgway, K.D., Manuszak, J.D., and Layer, P., 2002, Mesozoic sedimentary-basin development on the allochthonous Wrangellia composite terrane, Wrangell Mountains basin, Alaska: a long-term record of terrane migration and arc construction: Geological Society of America, Bulletin, v. 114, p. 693–717.

Van Hoesen, J.G., and Orndorff, R.L., 2004, A comparative SEM study on the micromorphology of glacial and nonglacial clasts with varying age and lithology: Canadian Journal of Earth Sciences, v. 41, p. 1123–1139.

Vos, K., Vandenberghe, N., and Elsen, J., 2014, Surface textural analysis of quartz grains by scanning electron microscopy (SEM): from sample preparation to environmental interpretation: Earth-Science Reviews, v. 128, p. 93–104.

Whalley, W.B., and Langway, C.C., 1980, A scanning electron microscope examination of subglacial quartz grains from Camp Century Core, Greenland: a preliminary study, Journal of Glaciology, v. 25, p. 125–132.

Witus, A.E., Branecky, C.M., Anderson, J.B., Szczuciński, W., Schroeder, D.M., Blankenship, D.D., and Jakobsson, M., 2014, Meltwater intensive glacial retreat in polar environments and investigation of associated sediments: example from Pine Island Bay, West Antarctica, Quaternary Science Reviews, v. 85, p. 99–118.

Received 14 August 2015; accepted 11 March 2016.